

# Geometrically frustrated, mechanical metamaterial membranes: Large-scale stress accumulation and size-selective assembly

Michael Wang<sup>1,\*</sup>, Sourav Roy<sup>2,†</sup>, Christian Santangelo<sup>2,‡</sup> and Gregory Grason<sup>1,§</sup>

<sup>1</sup>*Department of Polymer Science and Engineering,  
University of Massachusetts, Amherst, MA 01003*

<sup>2</sup>*Department of Physics, Syracuse University, NY 13210*

We study the effect of geometric frustration on dilational mechanical metamaterial membranes. While shape frustrated elastic plates can only accommodate non-zero Gaussian curvature up to size scales that ultimately vanish with their elastic thickness, we show that frustrated *metamembranes* accumulate hyperbolic curvatures up to mesoscopic length scales that are ultimately independent of the size of their microscopic constituents. A continuum elastic theory and discrete numerical model describe the size-dependent shape and internal stresses of axisymmetric, trumpet-like frustrated metamembranes, revealing a non-trivial crossover to a much weaker power-law growth in elastic strain energy with size than in frustrated elastic membranes. We study a consequence of this for the self-limiting assembly thermodynamics of frustrated trumpets, showing a several-fold increase in the size range of self-limitation of metamembranes relative to elastic membranes.

Geometric frustration occurs when a locally preferred structural motif cannot be realized globally [1]. In soft matter systems, from liquid crystals [2–4] to colloids [5–7] to filamentous assemblies [8–10], geometric frustration gives rise to the accumulation of elastic distortions at sizes much larger than the microscopic material elements [11–14]. Geometrically-frustrated elastic membranes are a well-studied, prototypical class of such systems [15], with broad applications to engineered and natural materials ranging from nano- to macro-scales. Frustration in elastic membranes derives from the elastic incompatibility between the preferred metric (i.e. intrinsic geometry) and the preferred curvatures (i.e. extrinsic geometry) of the membrane [16]. For example, the differential growth [17] or swelling [18, 19] of a sheet gives rise to a preferred non-Euclidean metric, which favors non-zero Gaussian curvature at the energetic expense of bending the sheet. These so-called *non-Euclidean plates* exhibit a complex spectrum of compromised equilibria, such as the undulating shapes of leaves [17] and torn plastic sheets [20]. On the other hand, for so-called *hyperbolic Euclidean shells*, the stress-free metric is Euclidean but the preferred curvature deforms the intrinsically flat shell to a saddle-like shape. [21].

Geometrically frustrated membranes are quite distinct from the case of externally imposed Gaussian curvature of plates and shells [22–24] in that the competition between metric (stretching) or shape (bending) in frustrated elastic membranes is *self-generating*, giving rise to remarkably non-linear, shape-adaptive, and size-dependent behavior. In hyperbolic Euclidean shells, narrow sheets accommodate the stretching cost of adopting a preferred Gaussian curvature, while wider sheets flatten to expel it to a narrow boundary layer at their edges [25, 26]. This size-dependent frustration drives the shape transition between helicoids to spiral ribbons observed in diverse systems such as Bauhinia seed pods [21], inorganic nanosheet ribbons [27, 28], and crystalline mem-

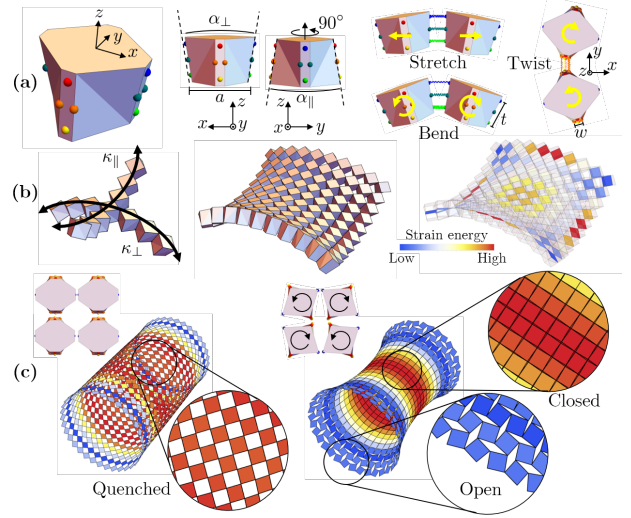


FIG. 1. (a) “Cuboid” subunit, elastic binding site locations (colored spheres), and pairwise deformation modes. (b) Preferred curvature of subunit rows (left) and negative Gaussian curvature 2D assembly (center) and elastic energy gradients, highlighted in cross-sectional cuts (right). (c) “Trumpet” metamembranes without (“quenched” or *stiff*) and with (*floppy*) a soft dilational mode.

branes of chiral amphiphiles [25, 29–31]. The *flattening size*  $\ell_{\text{flat}}$  [32] at which the transition occurs is set by the ratio of the elastic cost of bending to stretching in membranes, which vanishes with the microscopic thickness  $t$  [25, 33]. This implies that the size range  $\ell_{\text{flat}}$  and ability to accumulate Gaussian curvature is especially limited [34] for *self-assembled frustrated membranes*, since the accumulation of internal stresses with increasing size determines the range over which assemblies can “sense” and limit their dimensions [25, 29, 32].

In this Letter, we study the effect of geometric frustration in a mechanical metamaterial [35–37] membrane, dubbed a *metamembrane*, characterized by a bulk floppy

(i.e. zero-energy) dilational mode [38] in the absence of frustration. The existence of a floppy mode associated with the internal buckling of the metamembrane, fundamentally alters the nature and size-sensitivity of stress accumulation. We combine continuum theory and numerical simulations of 2D ordered metamembranes formed from subunits whose shape favors locally negative Gaussian curvature, with a corner-binding dilational mode permitting such geometry (Fig. 1). In the absence of frustration, such structures are known as conformal metamaterials [39, 40], and have been studied for their exotic 2D (in-plane) topological mechanics [41, 42] as well as engineered metamaterial responses [43, 44]. Here, we show that introducing geometric frustration through a preferred curvature internally stresses the otherwise floppy metamembrane. The local dilational modes screen the elastic costs of frustration [45], allowing the metamembrane to accumulate larger amounts of Gaussian curvature over a larger size-range. Unlike elastic membranes, this screening effect does not vanish with subunit size in the continuum limit, leading to a several fold increase in the thermodynamic self-limiting sizes of frustrated tubules. This opens up fundamentally distinct dimensions of structural control in programmable self-assemblies.

We consider a discrete-subunit model of hyperbolically frustrated metamembranes (Fig. 1) composed of 2D arrays of corner-binding, rigid, quasi-cuboidal subunits. In the absence of frustration, they exhibit a counter-rotation mechanism of alternating cuboids leading to 2D auxetic behavior. To introduce frustration, opposing corner edges are flared by angles  $+\alpha_{\parallel}$  and  $-\alpha_{\perp}$  (Fig. 1a). Ideal edge-to-edge binding along orthogonal rows gives rise to curvatures  $\kappa_{\parallel} \simeq \alpha_{\parallel}/a$  and  $\kappa_{\perp} \simeq \alpha_{\perp}/a$ , where  $a$  is the diagonal subunit width. Edges between neighboring units are held together by four pairs of binding sites—two vertically separated by  $t$  and two horizontally separated by  $w$ —connected by Hookean springs of stiffness  $k$ . As illustrated in Fig. 1a, distortions of these bonds determine the stiffnesses of the three modes of inter-unit mechanics: center-to-center stretching ( $\propto k$ ); inter-unit bending ( $\propto kt^2$ ); and inter-unit twisting ( $\propto kw^2$ ).

Pairwise interactions determine the collective mechanics of 2D sheets of these units (Fig. 1b) when targeting minimal surface shapes (e.g.  $\kappa_{\parallel} = -\kappa_{\perp}$ ). Notably, the inter-unit twist stiffness dramatically impacts the ability of frustrated metamembranes to accommodate non-zero Gaussian curvature. This is shown for the tubular assemblies in Fig. 1c with a self-closed hoop radius  $R = \kappa_{\perp}^{-1}$  and an axial *trumpet-like* flare [46]. When the twist mode is *stiff* (e.g.  $w \approx t$ ), the mechanism is effectively quenched and the equilibrium shape is only weakly perturbed from a uniform cylindrical shape near the edges. In contrast, for a *floppy* (e.g.  $w = 0$ ) twist mode, equilibrium shapes exhibit a hyperbolic curvature over the bulk of the assembly, as well as larger scale gradients in strain energy.

We can understand the shape and stress accumulation in frustrated metamembranes by way of a continuum Föppl-von Kármán like description of dilational metamaterial sheets [44] combined with the theory of hyperbolic Euclidean shells [25] (see Supplemental Material [47]). This model is described by an elastic energy  $\mathcal{W}$  composed of elastic strains  $\boldsymbol{\varepsilon}$  within the 2D array, the curvature tensor  $\boldsymbol{\kappa}$  of its out-of-plane shape, and a scalar field  $\Omega$  characterizing the amount of local dilation. The energy takes the form

$$\mathcal{W}(\boldsymbol{\varepsilon}, \boldsymbol{\kappa}, \Omega) = \int dA \left\{ \frac{1}{2} [(\lambda + \mu)(\varepsilon_{\text{dil}} - \Omega)^2 + 2\mu\varepsilon_{\text{dev}}^2] + \frac{B}{2} (\boldsymbol{\kappa} - \bar{\boldsymbol{\kappa}})^2 + \frac{C_{\text{mech}}}{2} |\Omega|^2 + \frac{C_{\nabla}}{2} |\nabla\Omega|^2 \right\}. \quad (1)$$

The bulk modulus  $(\lambda + \mu)$  couples the dilational strain  $\varepsilon_{\text{dil}} = \text{Tr} \boldsymbol{\varepsilon}$  to the twist mechanism, while deviatoric strains  $\boldsymbol{\varepsilon}_{\text{dev}} = \boldsymbol{\varepsilon} - \mathbb{1}\varepsilon_{\text{dil}}$  are uncoupled from the mechanism and penalized by a shear modulus  $\mu$ . The third term describes the bending cost with modulus  $B$  of a membrane deviating from its *target curvatures*

$$\bar{\boldsymbol{\kappa}} = \begin{pmatrix} \kappa_{\parallel} & 0 \\ 0 & -\kappa_{\perp} \end{pmatrix}. \quad (2)$$

The last two terms describe uniform and non-uniform actuation costs of the twist mechanism, where  $\nabla\Omega$  is its in-plane gradient. It is simple to show (see Supplemental Material) that the moduli are related to the subunit model (Fig. 1), with  $\lambda \propto \mu \propto k$ ,  $B \propto kt^2$ ,  $C_{\text{mech}} \propto k(w/a)^2$ , and  $C_{\nabla} \propto ka^2$ , consistent with planar dilational metamaterials [37, 40].

While it is straightforward to analytically solve for the shape equilibria of axisymmetric trumpets (see Supplemental Material), simple energy arguments suffice to explain the differences in how the elastic energy density,  $\omega \equiv \mathcal{W}/A$ , accumulates with length  $L$  for *stiff* ( $C_{\text{mech}} \approx k$ ) versus *floppy* ( $C_{\text{mech}} = 0$ ) metamembrane trumpets. For the stiff case ( $C_{\text{mech}} \approx k$ ), the mechanism is quenched ( $\Omega = 0$ ) at all relevant scales, and the bending energy dominates to maintain the target hyperbolic shape with Gaussian curvature  $K_{\text{G}} \approx -\kappa_{\perp}\kappa_{\parallel}$ . Gauss' theorem prescribes the dilational strain gradients to accommodate the non-Euclidean geometry  $\nabla^2\varepsilon_{\text{dil}} \simeq -K_{\text{G}}$ , which is solved by the quadratic growth of strain with axial distance  $z$  from the mid-point of the trumpet,  $\varepsilon_{\text{dil}}(z) = \varepsilon_{\text{dil}}(0) - K_{\text{G}}z^2/2$ , and a stretching energy density that grows as  $\omega(L \rightarrow 0) \sim YK_{\text{G}}^2L^4$ , where  $Y \propto 4\mu(\lambda + \mu)/(\lambda + 2\mu)$  is the (bare) 2D Young's modulus. This quartic growth with length (Fig. 2a) proceeds until trumpets reach a size where stretching exceeds the finite energy cost  $\omega(L \rightarrow \infty) \sim B\kappa_{\parallel}^2/2$  to unbend, or *flatten* the shape along the axial direction. This size is called the *flattening length*  $\ell_{\text{flat}}(\text{stiff}) = (B/Y)^{1/4}\kappa_{\perp}^{-1/2} \propto \sqrt{tR}$ , which is the well-known narrow size of the curved boundary layer in frustrated membranes [33].

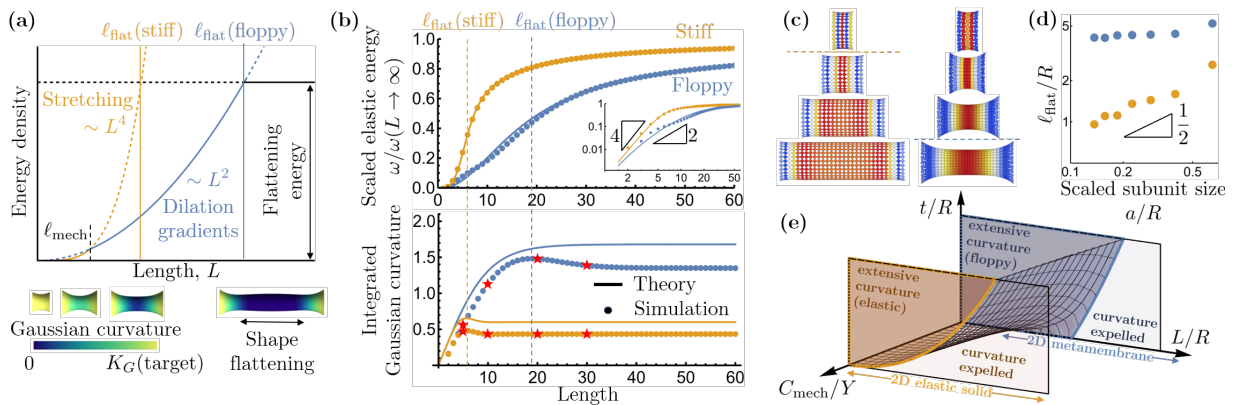


FIG. 2. (a) Schematic length-dependence (stretching, dilations, and flattening) of frustrated metatrumpets’ elastic energy. (b) Elastic energy per unit area  $\omega(L) = \mathcal{W}(L)/A$  and integrated Gaussian curvature as functions of  $L$  for  $\alpha_{\perp} = \pi/28$  and  $\alpha_{\parallel} = (3/4)\alpha_{\perp}$ , normalized by that of ( $L \rightarrow \infty$ ) limit. Solid lines show continuum predictions for stiff (orange) and floppy (blue) mechanism with  $\ell_{\text{mech}}/\ell_{\text{flat}}(\text{floppy}) \approx 0.25$  and  $C_{\text{mech}} = 0$ . Vertical dashed lines mark flattening transitions. (c) Ground states corresponding to the red stars in (b), with horizontal dashed lines delineating the onset of flattening. (d) Flattening length versus subunit size (for  $\kappa_{\parallel}/\kappa_{\perp} = 3/4$ ). (e) “Phase diagram” of mechanics of frustrated metatrumpets as function of reduced thickness, size, and mechanism stiffness, with the surface delineating ground states achieving 50% of the target curvature.

For the floppy case ( $C_{\text{mech}} = 0$ ), the twist mechanism is free to screen dilational strains via  $\Omega(z) \simeq \varepsilon_{\text{dil}}(z)$ , leading to a residual cost for twist gradients  $\partial_z \Omega \approx -K_G z$  that grows only quadratically with size as  $\omega \sim C_{\nabla} K_G^2 L^2$ . Dilational screening by twist (Fig. 2a) occurs for  $L \gtrsim \ell_{\text{mech}} = \sqrt{C_{\nabla}/Y} \propto a$ , beyond which the soft accumulation of elastic energy leads to a larger flattening size  $\ell_{\text{flat}}(\text{floppy}) = (B/C_{\nabla})^{1/2} \kappa_{\perp}^{-1} \propto (t/a)R$ . Interestingly, the screening of dilational strains in metamembranes leads to a quadratic power-law accumulation of frustration cost, akin to orientational strains in frustrated *liquid crystalline* membranes [13, 49].

We test this accumulation of elastic energy density with length  $N_{\parallel}$ , the number of subunits along the axial direction, for stiff versus floppy frustrated trumpets with a fixed geometry  $\kappa_{\parallel} = (3/4)\kappa_{\perp}$  in Fig. 2b (top). The comparison between continuum theory and discrete metamembranes shows a non-linear softening of elastic energy growth for floppy trumpets relative to stiff ones, with both smoothly saturating as  $L \rightarrow \infty$ . The inset shows an  $L^4$  growth of stretching energy for stiff trumpets, while for floppy trumpets the discrete subunit model suggests a power-law slightly weaker than the predicted  $L^2$ . We characterize the range of frustration accumulation in terms of integrated Gaussian curvature (Fig. 2b, bottom), which saturates just beyond a weak local maximum, marked by  $\ell_{\text{flat}}$ . Not only is the  $\ell_{\text{flat}}$  much larger for floppy trumpets compared to stiff ones, but so too is the total accumulated Gaussian curvature as  $L \rightarrow \infty$  (Fig. 2c). We highlight that, while  $\ell_{\text{flat}}(\text{stiff}) \sim t^{1/2}$  implies that the size scale of the  $K_G \neq 0$  zone vanishes as  $a \rightarrow 0$  for fixed aspect ratio  $a/t$ , the (larger)  $\ell_{\text{flat}}(\text{floppy}) \sim t/a$ , is independent of microscopic subunit size in this same limit (Fig. 2d).

Notably, for the distinct limit of  $a \gg t$ , arguably relevant to macroscopic “rigid panel” kirigami realizations of metasheets [37, 39], this theory suggests a much smaller range for  $\ell_{\text{flat}}(\text{floppy})$ , implying that unbending largely preempts the anomalous softening and curvature accumulation in such structures. In contrast, molecular or self-assembled membranes [27–30, 34], where the in-plane size and thickness are comparable ( $a \approx t$ ), constitute a unique class of frustrated 2D materials possessing the ability to “absorb” Gaussian curvature. This behavior is summarized in the 3D parameter space shown in Fig. 2e, where continuum theory is used to delineate conditions where non-zero Gaussian curvature is extensive in frustrated metatrumpets (i.e. at least 50% of its target value, see Supplemental Material). For standard 2D elastic solids lacking floppy modes (e.g.  $C_{\text{mech}} \approx Y$ ), Gaussian curvature is expelled to a boundary-layer of size  $\ell_{\text{flat}}(\text{stiff}) \sim t^{1/2}$ , akin to the Meissner effect of expelling magnetic fields from the interior of a superconductor. Hence, in the 2D limit of vanishing thickness  $t/R$ , the fraction of the elastic solid that absorbs Gaussian curvature vanishes for any macroscopic size. In the floppy limit ( $C_{\text{mech}} \rightarrow 0$ ), however, the metamembrane lacks one of the two characteristic moduli of a 2D elastic solid, exhibiting extensivity of Gaussian curvature even in the strictly 2D ( $t \rightarrow 0$ ) limit.

The much softer accumulation of elastic energy with size in frustrated floppy metamembranes has important consequences on their thermodynamic self-limiting states. In general, equilibrium self-limitation derives from a local minimum in the per-subunit free energy. This behavior has been reported in simulations of frustrated, trumpet-shaped crystalline membranes [46], notably inspired by a recently developed class of shape-

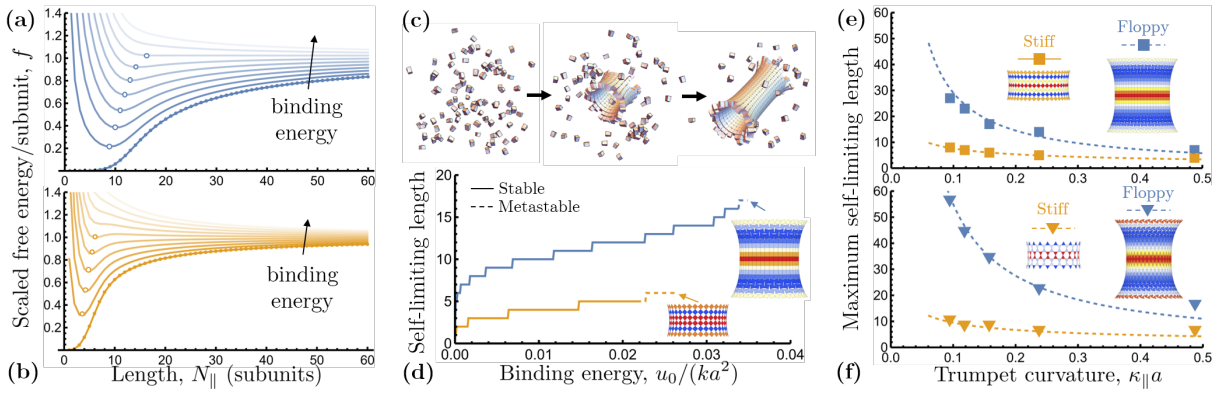


FIG. 3. Free energy per subunit, normalized by the flattened ( $L \rightarrow \infty$ ) case, for the assembly of (a) *stiff* and (b) *floppy* trumpets, shown schematically in (c), with target curvatures  $\kappa_{\perp} = \pi/30$  and  $\kappa_{\parallel} = (3/4)\kappa_{\perp}$ . Increasing transparency indicates increasing binding free energy,  $u_0$ , and open circles mark the self-limiting states. (d) Self-limiting length versus binding energy for stiff and floppy trumpets, with the largest equilibrium structure shown for each. Dashed lines are metastable local minima (i.e. thermodynamically unlimited regime). Maximum self-limiting length for trumpets with (e) square-twist and (f) Kagome metastructures, as functions of the target trumpet curvature  $\kappa_{\parallel}$  (with fixed ratio  $\kappa_{\parallel}/\kappa_{\perp} = 3/4$ ). Example structures shown have axial curvatures  $\kappa_{\parallel}a \approx 0.157$ . Solid and dashed lines show the scalings  $(\kappa_{\parallel}a)^{-1/2}$  for a stiff mode (orange) and  $(\kappa_{\parallel}a)^{-1}$  for a floppy mode (blue).

programmable DNA origami building blocks [50, 51]. However, the narrow range of elastic energy accumulation limits their self-limiting sizes to  $\lesssim 4 - 8$  subunits in width [34, 46]. Here, we consider the (ground state) per-subunit free energy of defect-free, axisymmetric metatrumpets, relevant in finite- $T$  simulations [46], which is parameterized by a binding free energy  $-u_0$  per bound corner,

$$f(N_{\parallel}) = -2u_0 + \frac{u_0}{N_{\parallel}} + \min_{N_{\perp}} [\omega(N_{\parallel}, N_{\perp})], \quad (3)$$

where the elastic energy density  $\omega(N_{\parallel}, N_{\perp})$  is minimized over hoop size ( $N_{\perp}$ ) for each trumpet length ( $N_{\parallel}$ ). As shown in the Supplemental Material, stiff trumpets favor hoop sizes close to those of the open structures (i.e.  $N_{\perp} = 2\pi R/a = 2\pi/(\kappa_{\perp}a)$ ), while floppy trumpets prefer larger hoop sizes that favor the maximal closure of the mechanism, increasing the selected hoop size to  $N_{\perp} = 2\pi R \sec \psi_{\max}/a$ , where  $\psi_{\max}$  is the maximal twist angle ( $\pi/4$  for square-twist), which requires excluded volume interactions to prevent subunit overlap. The per subunit cohesive cost  $u_0/N_{\parallel}$  of the open boundary in the second term drives the assembly to larger lengths, competing with the monotonically increasing per subunit elastic cost of frustration  $\omega$  with length. Figs. 3a-b show normalized per subunit free energy for stiff and floppy axisymmetric trumpets predicted by Eq. (3), for increasing binding strengths. While we are not considering finite- $T$  simulations of the length-selection process illustrated schematically in Fig. 3c, it is well-known that equilibrium finite-size assembly is controlled by the local minimum in the per-subunit assembly free energy [32]. For sufficiently small  $u_0$ ,  $f(N_{\parallel})$  has local minima at  $N_{\parallel}^*$ , indicating a thermodynamically favored self-limiting length.

Increasing binding strength increases that self-limiting size as well as the value of  $f(N_{\parallel}^*)$ . For sufficiently large  $u_0$ , the flattening of  $\omega(N_{\parallel})$  at large sizes leads either to  $f(N_{\parallel}^*) > f(N_{\parallel} \rightarrow \infty)$  (i.e. metastable finite length) or the vanishing of a local minimum, resulting in the thermodynamically unlimited growth of flattened trumpet assemblies. The dependence of the equilibrium self-limiting lengths on cohesive binding for stiff and floppy assemblies is shown in Fig. 3d. Notably, the softer and longer range of elastic energy accumulation in floppy assemblies results in a significantly enhanced self-limitation range. For the same target curvatures, the maximal self-limiting lengths for floppy trumpets extend up to 16 subunits in comparison to the modest upper limit of 5 subunits for stiff trumpets.

We compare the maximal self-limiting lengths for stiff and floppy metatrumpet assemblies of cuboidal subunits as a function of target curvature (for fixed ratio  $\kappa_{\parallel}/\kappa_{\perp}$ ) in Fig. 3e. Despite the absence of excluded volume in the continuum model, the upper limit of the self-limiting assembly size follows the same scaling as the flattening length  $\ell_{\text{flat}}$ , i.e., the maximal length grows more rapidly as the target curvature tends to zero for floppy trumpets ( $\sim \kappa_{\parallel}^{-1}$ ) than for stiff trumpets ( $\sim \kappa_{\parallel}^{-1/2}$ ). At the lowest curvature considered ( $\kappa_{\parallel}a \approx 0.094$ ), the maximal-size structures are composed of 1890 subunits for floppy trumpets, compared to only 432 subunits in the stiff ones.

While excluded volume effects do not apparently alter the scaling of elastic energy accumulation, we do find that micro-structural effects of saturating the dilational mechanism alter the quantitative enhancement of self-limiting size because the ratio  $\kappa_{\parallel}/\kappa_{\perp}$  controls the twist gradients that screen dilational strains (see Supplemental Mate-

rial). For sufficiently large  $\kappa_{\parallel}/\kappa_{\perp}$ , dilational screening exceeds the maximal twist  $\psi_{\max} = \pi/4$  for square-twist assemblies, leading to self-contacting zones. With this in mind, we consider a Kagome structure of rigid triangular units, which also exhibits a bulk floppy mode [52], but with an enhanced dilational range (4:1) relative to that of the square-twist (2:1). Hence, a simple redesign to flared triangular prismoidal sub-unit shapes (see Supplemental Material) exhibits the same frustrated metamembrane behavior (Fig. 3f) with enhanced self-limiting lengths for the same  $\kappa_{\parallel}/\kappa_{\perp}$ , up to a  $\sim 6$ -fold increase in the maximal length relative to the stiff case, with the largest structures considered possessing 5040 subunits.

In summary, the introduction of bulk “floppy” metamaterial modes into positionally ordered 2D membranes qualitatively changes the accumulation of internal stresses, and significantly extends the size range over which frustrated membranes accumulate Gaussian curvature. Hence, while frustrated “trumpets” [46] with standard solid elasticity exhibit hyperbolic curvature over a fraction  $\sim \sqrt{tR_0}/L$  of their length, which vanishes in the strictly 2D ( $t \rightarrow 0$ ) limit, frustrated metatrumpets exhibit curvature over a far more extensive, thickness-independent fraction  $\sim R_0/L$ . Although our specific model considers a dilational (i.e. auxetic) behavior, the elastic response of metasheets with a floppy shear mechanism [44] to Gaussian curvature implies that a more general class of metamembranes will similarly exhibit an anomalous absorption of Gaussian curvature, provided at least one of either their effective in-plane dilation or shear moduli vanish. The extensivity of curvature absorption has significant implications for molecular, self-assembled membranes, which are especially thin, and where elastic costs of in-plane and out-of-plane orientational gradients can be expected to be comparable (i.e.  $C_{\nabla} \sim B$ ). Hence these predictions apply to self-assembled metastructures of geometrically engineered nanoscale building blocks, such as auxetic square-twist assemblies of *de novo* proteins [53]. These results also demonstrate the significant potential to engineer assemblies that self-limit at large dimensions through not only the design of the “misfit” geometry of the subunits [54, 55], but also the introduction of floppy intra-assembly modes via their binding geometries. Notably, the triangular DNA origami subunit designs used in recent works demonstrating the curvature-programmable assembly of spheres [50] and cylinders [51] are ideally suited for realizing Kagome metamembrane assemblies of the type shown in (Fig. 3) implemented via vertex-to-vertex binding.

The authors are grateful to D. Hall for stimulating discussions on this model. This work was supported by US National Science Foundation through awards NSF DMR-2028885, DMR-239818, the Brandeis Center for Bioinspired Soft Materials, an NSF MRSEC, DMR-2011846 (M.W. and G.M.G.) and NSF DMR-2217543 (S.R. and C.D.S.). Computational studies were performed using

the UMass Cluster at the Massachusetts Green High Performance Computing Center.

---

\* mwang@mail.pse.umass.edu

† sroy08@syr.edu

‡ cdsantan@syr.edu

§ grason@umass.edu

- [1] J.-F. Sadoc and R. Mosseri, *Geometric Frustration*, 2nd ed. (Cambridge University Press, Cambridge, 2006).
- [2] D. C. Wright and N. D. Mermin, Crystalline liquids: the blue phases, *Rev. Mod. Phys.* **61**, 385 (1989).
- [3] I. Niv and E. Efrati, Geometric frustration and compatibility conditions for two-dimensional director fields, *Soft Matter* **14**, 424 (2018).
- [4] J. V. Selinger, Director deformations, geometric frustration, and modulated phases in liquid crystals, *Annual Review of Condensed Matter Physics* **13**, 49 (2022).
- [5] G. Meng, J. Paulose, D. R. Nelson, and V. N. Manoharan, Elastic instability of a crystal growing on a curved surface, *Science* **343**, 634 (2014).
- [6] W. T. M. Irvine, V. Vitelli, and P. M. Chaikin, Pleats in crystals on curved surfaces, *Nature* **468**, 947 (2010).
- [7] S. Li, R. Zandi, A. Travasset, and G. M. Grason, Ground states of crystalline caps: Generalized jellium on curved space, *Phys. Rev. Lett.* **123**, 145501 (2019).
- [8] I. R. Bruss and G. M. Grason, Non-euclidean geometry of twisted filament bundle packing, *Proc. Natl. Acad. Sci. USA* **109**, 10781 (2012).
- [9] A. Panaitescu, G. M. Grason, and A. Kudrolli, Persistence of perfect packing in twisted bundles of elastic filaments, *Phys. Rev. Lett.* **120**, 248002 (2018).
- [10] D. W. Atkinson, C. D. Santangelo, and G. M. Grason, Mechanics of metric frustration in contorted filament bundles: From local symmetry to columnar elasticity, *Phys. Rev. Lett.* **127**, 218002 (2021).
- [11] G. M. Grason, Perspective: Geometrically frustrated assembly, *J. Chem. Phys.* **145**, 110901 (2016).
- [12] S. Meiri and E. Efrati, Cumulative geometric frustration in physical assemblies, *Phys. Rev. E* **104**, 054601 (2021).
- [13] S. Meiri and E. Efrati, Cumulative geometric frustration and superextensive energy scaling in a nonlinear classical *xy*-spin model, *Phys. Rev. E* **105**, 024703 (2022).
- [14] N. W. Hackney, C. Amey, and G. M. Grason, Dispersed, condensed, and self-limiting states of geometrically frustrated assembly, *Phys. Rev. X* **13**, 041010 (2023).
- [15] E. Sharon and E. Efrati, The mechanics of non-euclidean plates, *Soft Matter* **6**, 5693 (2010).
- [16] J. Gemmer and S. C. Venkataramani, Shape transitions in hyperbolic non-euclidean plates, *Soft Matter* **9**, 8151 (2013).
- [17] H. Liang and L. Mahadevan, The shape of a long leaf, *Proc. Natl. Acad. Sci. USA* **106**, 22049 (2009).
- [18] Y. Klein, E. Efrati, and E. Sharon, Shaping of elastic sheets by prescription of non-euclidean metrics, *Science* **315**, 1116 (2007).
- [19] J. Kim, J. A. Hanna, M. Byun, C. D. Santangelo, and R. C. Hayward, Designing responsive buckled surfaces by halftone gel lithography, *Science*, 1201 (2012).
- [20] E. Sharon, B. Roman, and H. L. Swinney, Geometrically driven wrinkling observed in free plastic sheets and

- leaves, *Phys. Rev. E* **75**, 046211 (2007).
- [21] S. Armon, E. Efrati, R. Kupferman, and E. Sharon, Geometry and mechanics in the opening of chiral seed pods, *Science* **333**, 1726 (2011).
- [22] J. Hure, B. Roman, and J. Bico, Stamping and wrinkling of elastic plates, *Phys. Rev. Lett.* **109**, 054302 (2012).
- [23] B. Davidovitch, Y. Sun, and G. M. Grason, Geometrically incompatible confinement of solids, *Proc. Natl. Acad. Sci.* **116**, 1483 (2018).
- [24] I. Tobasco, Y. Timounay, D. Todorova, G. C. Leggat, J. D. Paulsen, and E. Katifori, Exact solutions for the wrinkle patterns of confined elastic shells, *Nat. Phys.* **18**, 1099 (2022).
- [25] S. Armon, H. Aharoni, M. Moshe, and E. Sharon, Shape selection in chiral ribbons: from seed pods to supramolecular assemblies, *Soft Matter* **10**, 2733 (2014).
- [26] D. Grossman, E. Sharon, and H. Diamant, Elasticity and fluctuations of frustrated nanoribbons, *Phys. Rev. Lett.* **116**, 258105 (2016).
- [27] F. Serafin, J. Lu, N. Kotov, K. Sun, and X. Mao, Frustrated self-assembly of non-euclidean crystals of nanoparticles, *Nat. Commun.* **12**, 4925 (2021).
- [28] D. Monego, S. Datta, D. Grossmann, M. Krapez, P. Bauer, A. Hubley, J. Margueritat, B. Mahler, A. Widmer-Cooper, and B. Abécassis, Ligand-induced incompatible curvatures control ultrathin nanoplatelet polymorphism and chirality, *Proc. Natl. Acad. Sci. USA* **121**, e2316299121 (2024).
- [29] R. Ghafouri and R. Bruinsma, Helicoid to spiral ribbon transition, *Phys. Rev. Lett.* **94**, 138101 (2005).
- [30] M. Zhang, D. Grossman, D. Danino, and E. Sharon, Shape and fluctuations of frustrated self-assembled nano ribbons, *Nat. Comm.* **10**, 3535 (2019).
- [31] R. L. B. Selinger, J. V. Selinger, A. P. Malanoski, and J. M. Schnur, Shape selection in chiral self-assembly, *Phys. Rev. Lett.* **93**, 158103 (2004).
- [32] M. F. Hagan and G. M. Grason, Equilibrium mechanisms of self-limiting assembly, *Rev. Mod. Phys.* **93**, 025008 (2021).
- [33] E. Efrati, E. Sharon, and R. Kupferman, Buckling transition and boundary layer in non-euclidean plates, *Phys. Rev. E* **80**, 016602 (2009).
- [34] D. M. Hall, M. J. Stevens, and G. M. Grason, Building blocks of non-euclidean ribbons: Size-controlled self-assembly via discrete frustrated particles, *Soft Matter* **19**, 858 (2023).
- [35] K. Bertoldi, V. Vitelli, J. Christensen, and M. van Hecke, Flexible mechanical metamaterials, *Nature Reviews Materials* **2**, 1 (2017).
- [36] C. D. Santangelo, Extreme Mechanics: Self-Folding Origami, *Annual Review of Condensed Matter Physics* **8**, 165 (2017).
- [37] Y. Zheng, I. Niloy, I. Tobasco, P. Celli, and P. Plucinsky, Modelling planar kirigami metamaterials as generalized elastic continua, *Proceedings of the Royal Society A: Mathematical, Physical and Engineering Sciences* **479**, 20220665 (2023).
- [38] K. Sun, A. Souslov, X. Mao, and T. C. Lubensky, Surface phonons, elastic response, and conformal invariance in twisted kagome lattices, *Proceedings of the National Academy of Sciences* **109**, 12369 (2012).
- [39] Y. Zheng, I. Niloy, P. Celli, I. Tobasco, and P. Plucinsky, Continuum field theory for the deformations of planar kirigami, *Phys. Rev. Lett.* **128**, 208003 (2022).
- [40] M. Czajkowski, C. Coulais, M. van Hecke, and D. Z. Rocklin, Conformal elasticity of mechanisms-based metamaterials, *Nat. Comm.* , 211 (2022).
- [41] J. Paulose, A. S. Meeussen, and V. Vitelli, Selective buckling via states of self-stress in topological metamaterials, *Proceedings of the National Academy of Sciences* **112**, 7639 (2015).
- [42] X. Mao and T. C. Lubensky, Maxwell lattices and topological mechanics, *Annual Review of Condensed Matter Physics* **9**, 413 (2018).
- [43] M. Konaković, K. Crane, B. Deng, S. Bouaziz, D. Piker, and M. Pauly, Beyond developable: computational design and fabrication with auxetic materials, *ACM Trans. Graph.* **35** (2016).
- [44] S. Roy and C. D. Santangelo, Curvature screening in draped mechanical metamaterial sheets, *Soft Matter* **19**, 8150 (2023).
- [45] N. S. Livne, A. Schiller, and M. Moshe, Geometric theory of mechanical screening in two-dimensional solids, *Phys. Rev. E* **107**, 055004 (2023).
- [46] B. Tyukodi, F. Mohajerani, D. M. Hall, G. M. Grason, and M. F. Hagan, Thermodynamic size control in curvature-frustrated tubules: Self-limitation with open boundaries, *ACS Nano* **16**, 9077 (2022).
- [47] See Supplemental Material at [url] for details regarding discrete particle simulations and the derivation of the continuum theory, which includes Ref. [48].
- [48] J. D. Weeks, D. Chandler, and H. C. Anderson, Role of repulsive forces in determining the equilibrium structure of simple liquids, *J. Chem. Phys.* **54**, 5237 (1971).
- [49] D. Nelson and L. Peliti, Fluctuations in membranes with crystalline and hexatic order, *Journal de physique* **48**, 1085 (1987).
- [50] C. Sigl, E. M. Willner, W. Engelen, J. A. Kretzmann, K. Sachenbacher, A. Liedl, F. Kolbe, F. Wilsch, S. A. Aghvami, U. Prozter, M. F. Hagan, S. Fraden, and H. Dietz, Programmable icosahedral shell system for virus trapping, *Nat. Mater.* **20**, 1281 (2021).
- [51] D. Hayakawa, T. E. Videbaek, D. M. Hall, H. Fang, C. Sigl, E. Feigl, H. Deitz, S. Fraden, M. F. Hagan, G. M. Grason, and W. B. Rogers, Geometrically programmed self-limiting assembly of tubules using dna origami colloids, *Proc. Natl. Acad. Sci. USA* **119**, e2207902119 (2022).
- [52] X. Mao, Q. Chen, and S. Granick, Entropy favours open colloidal lattices, *Nature Materials* **12**, 217 (2013).
- [53] R. Alberstein, Y. Suzuki, F. Paesani, and F. Tezcan, Engineering the entropy-driven free-energy landscape of a dynamic nanoporous protein assembly, *Nature Chemistry* **10**, 732–739 (2018).
- [54] M. Lenz and T. A. Witten, Geometrical frustration yields fibre formation in self-assembly, *Nat. Phys.* **13**, 1100 (2017).
- [55] I. R. Spivack, D. M. Hall, and G. M. Grason, Stress accumulation versus shape flattening in frustrated, warped-jigsaw particle assemblies, *New. J. Phys.* **24**, 063023 (2022).